Analysis of Regular Perforated Metal Ceiling Tiles

Uğur Albayrak and Mustafa Halûk Saraçoğlu

***Abstract*—Metal ceiling tiles can be used for a variety of space, including commercial, office and other public spaces. They are widely used for suspending ceilings and other architectural applications in a range of different perforation patterns to suit both mechanical and aesthetic requirements. These perforated panels made of steel, aluminum, bras, etc. are also known as stamping plates or sheets depending on its thickness and area of usage. In this study, perforated ceiling tiles are modelled as rectangular thin plates with various hole patterns which are simply supported on all its boundaries. The main idea is to find out the effect of the holes on the bending behaviour of the perforated plate which is the governing attitude of a ceiling tile. The other parameters which determined about the behaviour of the plates are deflection, moments and stresses. The analyses were performed on various models systematically by number, diameter and location of holes. As a result of these analyses the relationships between the applied force and maximum values of internal forces have been calculated by using APDL codes based on Finite Element Method to find out the optimum hole pattern. According to analysis results; 3D graphics are developed to design proper hole patterns for Regular Perforated Metal Ceiling Tiles.**

***Index Terms*—Circular holes, finite element method, plate, regular perforated.**

I. Introduction

The perforated plates are being used for a wider variety of different aims such as acoustical wall and ceiling panels, ceiling panels and lightweight decorative stuff to load-bearing structural elements, hand rail infill panels, sun shading devices, point-of-purchase displays and many others. Perforated plates are today used for a wider variety of applications than ever before. Unlike solid plate, perforated plate is permeable and transparent which makes it more versatile. It can be used for filtering, separation, protection, soundproofing, decorating, washing and drying.

Perforated panels are very versatile and convenient items to achieve sustainable design objectives. Especially choosing of perforation patterns and open area percentage is considered for unique and specific projects in terms of weight reduction, interior airflow controls and energy saving (Fig. 1.)

Plate with a circular hole at the center, bending of a square plate with a circular hole examined in the most important reference for plates and shells by Timoshenko and Woinowsky-Krieger [1]. O'Donnell and Langer published an article that describes a method for calculating stresses and deflections in perforated plates with a triangular penetration pattern [2]. Alshaya, Hunt and Rowlands determined the stress and strain concentrations in orthotropic composite plates with a circular hole in thickness direction by finite element method in their studies [3]. Kılıç, Ekici and Bedir investigated about using perforated plates for ballistic protection [4]. Radisavljevic *et al.* presented experimental results for the ballistic performance of perforated plates and optimize the geometrical characteristics of these structures [5]. Woo, Leissa and Kang analyzed about exact solutions for stresses, strains, displacements, and the stress concentration factors of a perforated rectangular plate by a circular hole subjected to in-plane bending moment on two opposite edges by two-dimensional theory of elasticity using the Airy stress function [6]. In their study, Zhou *et al.* presented mechanical and dynamical behaviors of perforated plates for the design and optimization purpose [7]. Pedersen, Olthuis and Bergveld developed an alternative approach to the modelling of perforated plates [8]. Atanasiu and Sorohan are investigated the stress distribution and displacement for a simply supported circular plate perforated by 96 holes arranged in a grid of squares and loaded through a central concentrated force or by uniformly distributed load [9]. Mei *et al.* established 3D simulation models of eighteen-type perforated plates that have different open-pore number [10]. Saraçoğlu and Albayrak analyzed perforated plates in their studies [11], [12].

Fig. 1. Perforated plate examples.

II. Material and Methods

The bending and twisting moments acting on the element per unit length is denoted by M_r , M_t and M_{rt} are shown in Fig. 2. To express these moments by *w* -the deflection of the plate- it is assumed that the x axis coincides with the radius *r* [1].

Manuscript received January 23, 2018; revised July 12, 2018.

Uğur Albayrak is with Eskisehir Osmangazi University, Dept. of Civil Engineering, Eskisehir, Turkey (corresponding author: Uğur Albayrak e-mail: albayrak@ogu.edu.tr).

Mustafa Halûk Saraçoğlu is with Dumlupınar University, Dept. of Civil Engineering, Kutahya, Turkey (e-mail: mhaluk.saracoglu@dpu.edu.tr).

DOI: 10.7763/IJET.2018.V10.1099

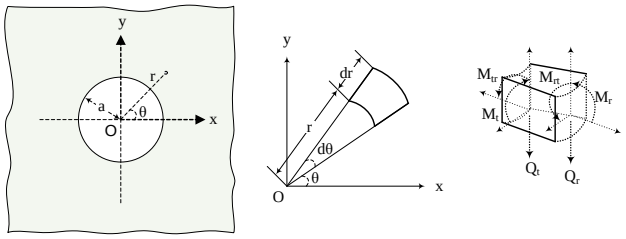

Fig. 2. Polar coordinates and positive directions of moments on a plate.

The moments can be expressed as (1):

$$M_r = -D\left(\frac{\partial^2 w}{\partial x^2} + \upsilon\frac{\partial^2 w}{\partial y^2}\right)_{\theta=0} = -D\left[\frac{\partial^2 w}{\partial r^2} + \upsilon\left(\frac{1}{r}\frac{\partial w}{\partial r} + \frac{1}{r^2}\frac{\partial^2 w}{\partial \theta^2}\right)\right]$$
$$M_t = -D\left(\frac{\partial^2 w}{\partial y^2} + \upsilon\frac{\partial^2 w}{\partial x^2}\right)_{\theta=0} = -D\left[\frac{1}{r}\frac{\partial w}{\partial r} + \frac{1}{r^2}\frac{\partial^2 w}{\partial \theta^2} + \upsilon\frac{\partial^2 w}{\partial r^2}\right]$$
$$M_{rt} = (1-\upsilon)D\left(\frac{\partial^2 w}{\partial x \partial y}\right)_{\theta=0} = (1-\upsilon)D\left[\frac{1}{r}\frac{\partial^2 w}{\partial r \partial \theta} - \frac{1}{r^2}\frac{\partial w}{\partial \theta}\right]$$

where;

$$D = \frac{E\,h^3}{12(1-\upsilon^2)}$$

Is the flexural rigidity, E is the Young's modulus, h is the thickness of the plate, ν is the Poisson's ratio and *w* is the vertical deflection of the plate.

In a uniform state of stress the bending moments of the plate is $M'_x = M_0$ and $M'_y = 0$. Deflection surface of the plate can be expressed as (2):

$$w = -\frac{M_0}{2D}\left\{\frac{r^2}{2(1-\upsilon^2)}\left[1-\upsilon+(1+\upsilon)\cos 2\theta\right] + a^2\left[A\log r + \left(B + C\frac{a^2}{r^2}\right)\cos 2\theta\right]\right\}$$

The action of the stresses along the periphery of the hole is dependent on the external couples and forces which are readily obtained by the Equation 3 as follows:

$$(M'_r)_{r=a} = \frac{M_0}{2}(1+\cos 2\theta) \quad (3)$$
$$(V'_r)_{r=a} = \frac{M_0}{a}\cos 2\theta$$

Deflection surface yields the following stress resultants on the periphery of the hole.

$$(M''_r)_{r=a} = -\frac{M_0}{2}\left\{(1-\upsilon)A + \left[4\upsilon B - 6(1-\upsilon)C\right]\cos 2\theta\right\} \quad (4)$$
$$(V''_r)_{r=a} = \frac{M_0}{a}\left[(6-2\upsilon)A + 6(1-\upsilon)C\right]\cos 2\theta$$

Equations (3) and (4) for M_r contain a constant term as well as a term proportional to cos 2, while both expressions for V_r contain only one term, three equations are needed to satisfy the required conditions $M_r' + M_r'' = 0$ and $V_r' + V_r'' = 0$ on the periphery of the hole.

$$M_t = -M_0\left[1 - \frac{2(1+\upsilon)}{3+\upsilon}\cos 2\theta\right] \quad (5)$$
$$Q_t = \frac{4M_0}{(3+\upsilon)a}\sin 2\theta$$

Resolving these equations with respect to the unknown coefficients A, B and C resultants along the periphery of the plate can be calculated using the Equation (5).

A. Perforated Thin Plates

As for the base material, the tiles are available in aluminum (0.6 / 0.7 mm thick), galvanized steel (0.5 mm thick), anodized aluminum (mirror look) (0.75 mm thick) or vinyl laminated gypsum (0.8 mm thick). Tiles generally come in the standard sizes of 300x300 mm, 300x600 mm, 600x600 mm but in case of special orders, they are available in other sizes upon request. Additional hangers should be reserved in case of increasing lighting and ventilating accessory weights. Runners are available in two base widths, namely T-24 and T-15. RAL 9001, 9002, 9003, 9006, 9010, 9016 and 7047 are the standard colors for ULTIMA lay-in systems. Other colors of RAL can be offered upon request.

Fig. 3. Thin rectangular plates with multiple circular holes.

Metal Ceiling Tiles which are commonly described as thin plates with multiple circular holes are made of superior-quality aluminum or steel plates with the processes of punching, forming, cleaning and washing (Figure 3).

B. Rectangular Plate Models

A plate is a structural element with planform dimensions that are large compared to its thickness and is subjected to loads that cause bending deformation in addition to stretching. In most cases, the thickness is no greater than one-tenth of the smallest in-plane dimension. Because of the smallness of thickness dimension, it is often not necessary to model them using 3D elasticity equations. Simple 2D plate theories can be developed to study the deformation and stresses in plate structures [13].

In this study perforated rectangular thin plates can be modelled as simply supported plates with multiple circular holes under self-weights. From day to day importance of computers increases in today's engineering. There were so much structural analysis softwares produced by these electronic brains that have to utilize as a tool. ANSYS is general packaged software that uses finite element method and also has a special code language. APDL stands for ANSYS Parametric Design Language, a scripting language that can be used to automate common tasks or build a model in terms of parameters (variables). In this study, APDL codes are developed to create and analyze the plate models systematically [14]-[16].

"Shell93" element is chosen to solve the analyzed plate examples in this study. Load is assumed under self-weights. The rectangular plates in this study are modelled with simply-supported boundary conditions on four sides. They meshed with triangular free mesh. In free meshing operations, no special requirements restrict the model. The element shapes used will depend on meshing areas. For area meshing, a free mesh can consist of only triangular elements. Finite element mesh dimensions are almost the same in all of the examples. One side of each mesh element is formed approximately equal to thickness of the plate because total numbers of mesh elements are almost same in each model.

The perforated rectangular thin plates with multiple circular holes examined to different number, radius and locations. In the models; x length of the plate is named as "b" and y length of the plate is named as "a" Figure 4. Two main models was created, whose x length is being twice of the length y and three times of the length y. Plate thickness is dependent to "a" so that the analysis results could be compared properly. Total surface areas of holes are exactly same for each model. Because of total hole area is equal in all models, the volume and so weight of the plates are exactly same and all models were analyzed under the same loads.

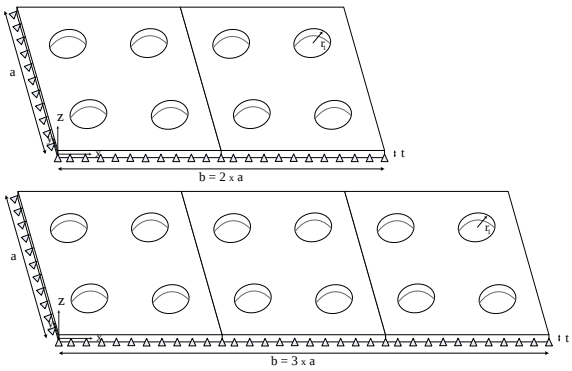

Fig. 4. Geometry of a regular perforated rectangular plate.

In first main model x length "b" is twice of the y length "a" so that aspect ratio is 1 / 2. There were ten sub models in first main model. In first sub model with 8 holes that are placed symmetrically along the lines x=b/2 and y= a/2 are examined (Fig. 5a). The radius of all holes are r=a/8 , where "a" is a one side of the rectangular plate and "r" is the radius of the hole. The centers of the holes are placed systematically as shown in Fig. 4.

In the second sub model, the rectangular plate is divided into 4 pieces with an edge "a/2" on y axis and "b/2" in x axis then the first model is scaled down and placed in each area. So the rectangular plate model with 32 holes whose radius (r2) are "a/16" was created (Fig. 5b). In third model, the rectangular plate is divided into 9 pieces with an edge "a/3" on y axis and "b/3" in x axis then the first model is scaled down and placed in each area. So the rectangular plate model with 72 holes whose radius (r3) is "a/24" was created (Fig. 5c).

The new plate models with different number of holes and radius are created by converting into a series on a regular basis up to model with 800 holes (Fig. 5).

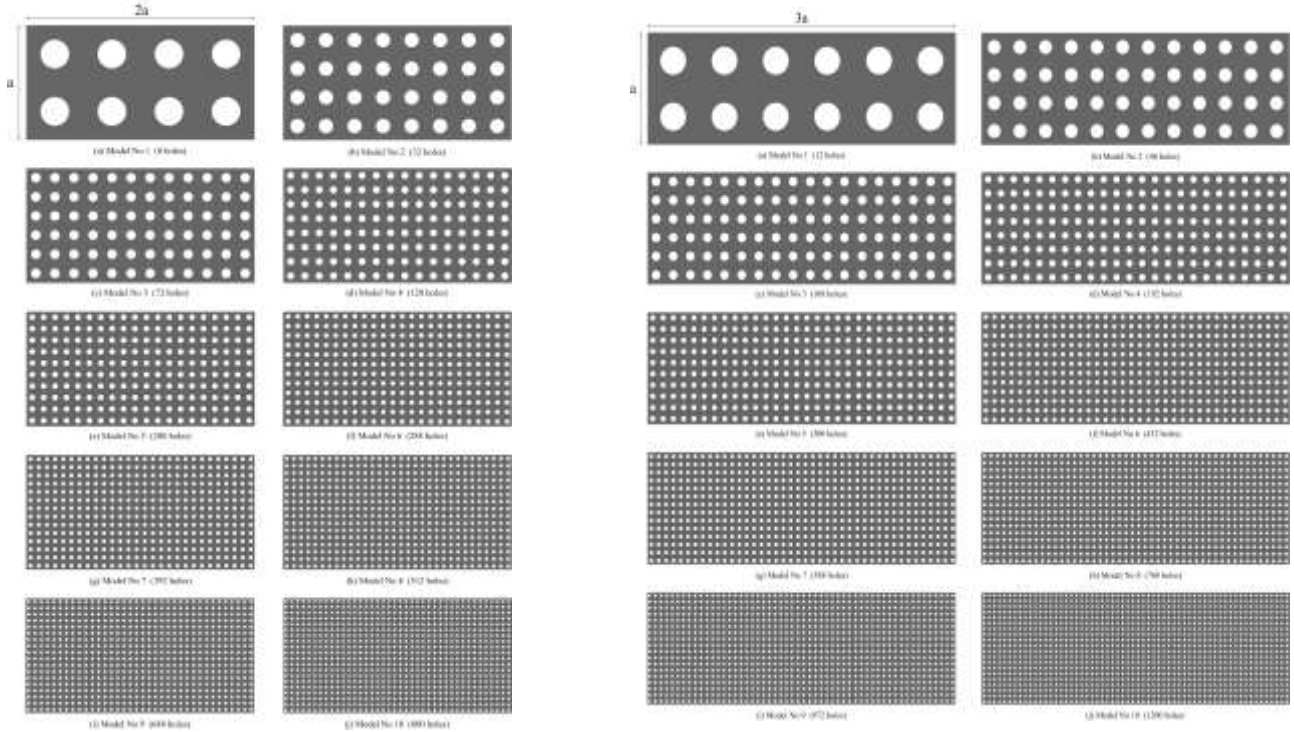

Fig. 5. Rectangular plate models with multiple circular holes for aspect ratio 1 / 2 and 1 / 3.

Changing the length of a rectangular plate "a", the plate thickness "t" is not to be constant and changes depends on "a". However a/t ratio is constant and equals to 150.

For each model, the total hole area of each plate is constant and equal to $\pi.a^2/8$ that are independent of "r" and number of holes, where "a" is the y length of the rectangular plate. The radius of the holes are the design variable furthermore the radius is constrained between a minimum value of r=a/80 and maximum value of r=a/8 for 10 different models (Table I).

TABLE I: HOLE NUMBERS IN FIRST MAIN MODEL (ASPECT RATIO = 1 / 2)

Sub model No	Number of holes	Radius (r)	Total hole area
1	8	a / 8	$8.\pi.(a/8)^2$
2	32	a / 16	$32.\pi.(a/16)^2$
3	72	a / 24	$72.\pi.(a/24)^2$
4	128	a / 32	$128.\pi.(a/32)^2$
5	200	a / 40	$200.\pi.(a/40)^2$
6	288	a / 48	$288.\pi.(a/48)^2$
7	392	a / 56	$392.\pi.(a/56)^2$
8	512	a / 64	$512.\pi.(a/64)^2$
9	648	a / 72	$648.\pi.(a/72)^2$
10	800	a / 80	$800.\pi.(a/80)^2$
n	$8.n^2$	a /(8.n)	$\pi.a^2/8$

C. Computational Analysis of Plate Models

In first model (aspect ratio 1 / 2) ; Sub Model No.2 plate which length is 1200 mm and width is 600 mm and thickness is 4 mm and has 32 circular holes examined statically under self-weights with gravity of g = 9810 mm/sn^2. The plate is made out of steel according to ASTM A992, with density of ρ = 7.697e-8 N/mm^3, modulus of elasticity 199948 N/mm^2 and Poisson's ratio of 0.3.

Stress and displacement analysis of perforated rectangular plates are examined. To this purpose examples are implemented in APDL codes in ANSYS. Linear elastic isotropic material properties of plate are defined. The program automatically creates the triangular free mesh using Shell93 element and the mesh around the holes refined. The boundary conditions for simply supported edges are defined. The self-weight of the plate is assumed as the static load distributed over the surface uniformly. The vertical displacement field of the plate in this section with aspect ratio 1 / 2 is given by contour plots shown at Figure 6. Deflections on the defined path passed from x = b / 2 is also given in Figure 6. The maximum deflection value is -4.357 mm occurs at the point x = b / 2 and y = a / 2 of given plate.

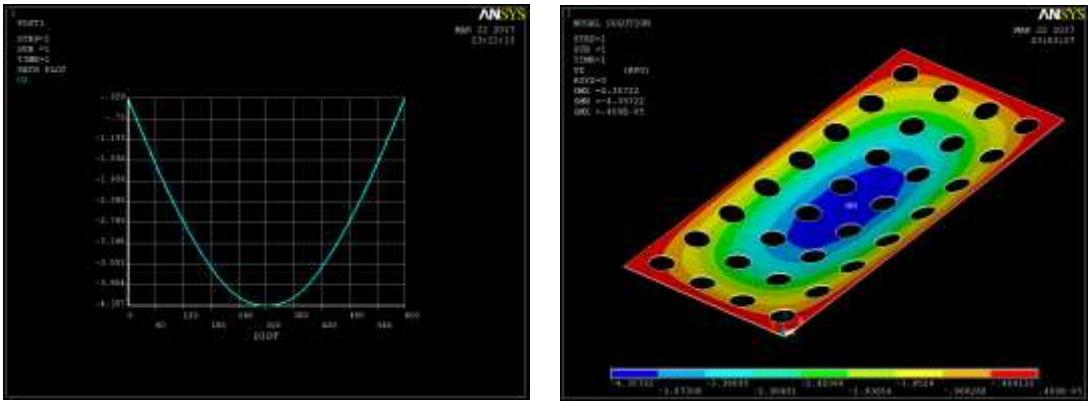

Fig. 6. Vertical displacement field of 1200x600x4 mm rectangular perforated plate with 32 circular holes.

The stress results on the defined paths passed from x = b / 2 and y = a / 2 are given in Fig. 7.

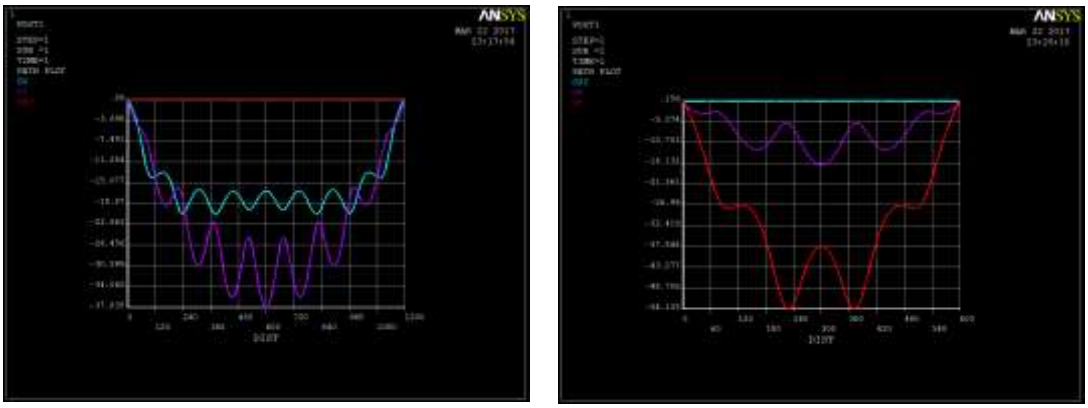

Fig. 7. Stress results on the paths of 1200x600x4 mm rectangular perforated plate with 32 circular holes.

The solved plate size of 1200x600x4 mm with 32 circular holes for Sub Model No.2 is also analyzed for 10 models with different number of holes.

III. Results and Discussion

Static analysis in ANSYS is performed to evaluate the influence of radius and number of holes. All of the plate examples were analyzed statically under self-weights and the results of the analysis are used to develop useful and practical graphics for the midpoint deflection of plates with multiple circular holes.

The analysis procedures reproduced for different "a" values which is y length of rectangular plate. For different plate length "a" as 100 mm, 200 mm, 300 mm, 400 mm and 500 mm respectively; 10 sub models with different number of holes are analyzed and midpoint deflections respect to number of holes and plate width are presented (Table II).

TABLE II: Midpoint Deflections (W_0) of Perforated Rectangular Plates with Aspect Ratio 1 / 2 (mm)

		a (mm)						
		100	***200***	***300***	***400***	***500***		
Number of Holes	**8**	-0.11578	-0.46313	-1.04200	-1.85250	-2.89460	**1**	**Model No**
	32	-0.12103	-0.48414	-1.08930	-1.93650	-3.02590	**2**	
	72	-0.12225	-0.48899	-1.10020	-1.95600	-3.05620	**3**	
	128	-0.12283	-0.49133	-1.10550	-1.96530	-3.07080	**4**	
	200	-0.12322	-0.49289	-1.10900	-1.97160	-3.08060	**5**	
	288	-0.12354	-0.49416	-1.11190	-1.97660	-3.08850	**6**	
	392	-0.12382	-0.49526	-1.11430	-1.98100	-3.09540	**7**	
	512	-0.12407	-0.49626	-1.11660	-1.98500	-3.10160	**8**	
	648	-0.12430	-0.49722	-1.11870	-1.98890	-3.10760	**9**	
	800	-0.12451	-0.49803	-1.12060	-1.99210	-3.11270	**10**	
		200	***400***	***600***	***800***	***1000***		
		b (mm)						

As a result of the analysis for 10 sub models, for any size of rectangular plate, the number of holes increases the midpoint deflection also increases although total hole area is equal in all models. In other words, number of holes for any plate is proportional to midpoint deflection but it is not linear. First part of the graphic; deflections increase very rapidly up to 128 holes, beyond this point hole numbers increase, the deflections also begin to increase slightly. Number of holes increase, the variation of the midpoint deflections decrease asymptotically after 128 holes so analyzing 10 models is sufficient for the results of the study. A linear normalization procedure is used to eliminate the differences between maximum displacement values on direction Z since therefore general graphics were proposed for each model depending on plate dimensions. Midpoint deflections of perforated rectangular plates with aspect ratio 1 / 2 normalized for all models with Equation 6 and graphed in Fig. 8.

$$W_{0\_normalized} = W_{0\_model} / W_{0\_model\_1} \quad (6)$$

On the other hand, plate dimensions with same number of holes increase, midpoint deflections also increase as expected because of plate weight also increase.

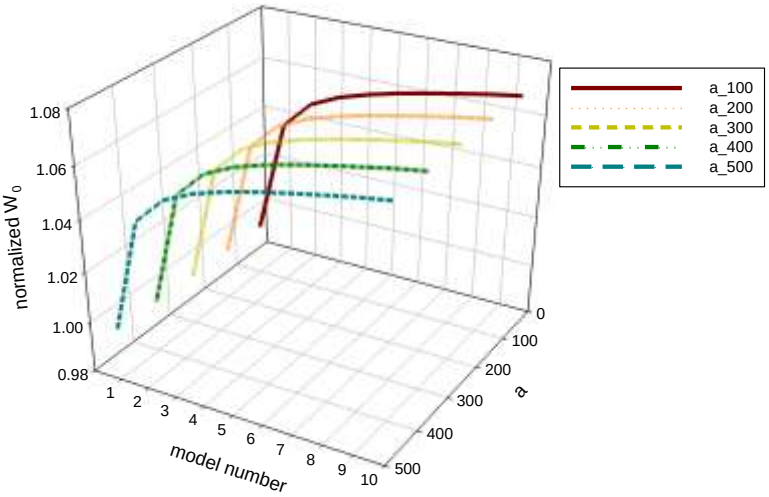

Fig. 8. Normalized midpoint deflections of perforated rectangular plates with aspect ratio 1 / 2.

All of the midpoint deflections are divided by the surface area of related rectangular plates and ratio values in (1/mm) for all models are calculated shown in Table III. These ratios are independent from plate dimensions so one side of rectangular plate changes the ratios remain constant for any number of holes (Table III). As a result the midpoint deflections could be estimated for different rectangular plate dimensions easily from the graphic (Fig. 9).

TABLE III: MIDPOINT DEFLECTIONS DIVIDED BY SURFACE AREA OF PLATE (10^{-6}/MM)

		a (mm)						
		100	***200***	***300***	***400***	***500***		
Number of Holes	**8**	-7.203	-7.204	-7.203	-7.203	-7.204	**1**	**Model No**
	32	-7.530	-7.530	-7.530	-7.530	-7.530	**2**	
	72	-7.606	-7.606	-7.606	-7.606	-7.606	**3**	
	128	-7.642	-7.642	-7.642	-7.642	-7.642	**4**	
	200	-7.666	-7.666	-7.666	-7.667	-7.667	**5**	
	288	-7.686	-7.686	-7.686	-7.686	-7.686	**6**	
	392	-7.704	-7.703	-7.703	-7.703	-7.703	**7**	
	512	-7.719	-7.719	-7.719	-7.719	-7.719	**8**	
	648	-7.733	-7.734	-7.733	-7.734	-7.734	**9**	
	800	-7.747	-7.746	-7.747	-7.746	-7.746	**10**	
		200	***400***	***600***	***800***	***1000***		
		b (mm)						

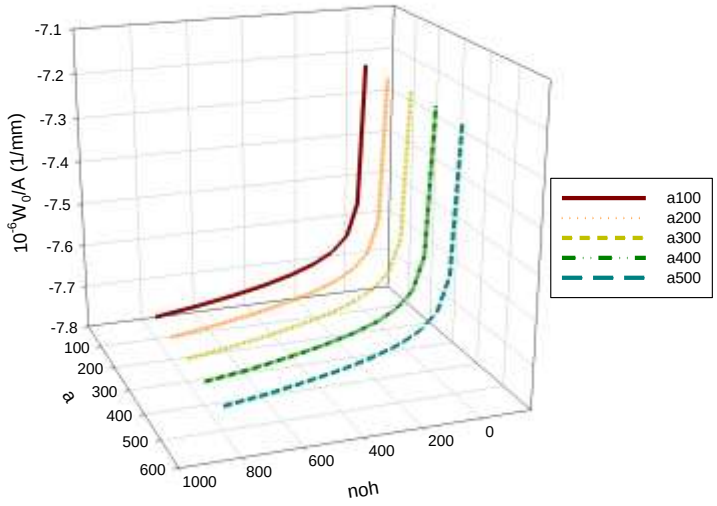

Fig. 9. Ratio of midpoint deflections to surface areas for all models (aspect ratio 1 / 2).

IV. CONCLUSION

Stresses, moments and deflections of perforated rectangular thin plates are statically analyzed under their self-weights in this study. To this purpose developed ten sub models for two main models are implemented in APDL codes in ANSYS package software.

Sub models are consists of different y lengths of rectangular plates. For different plate length "a" as 100 mm, 200 mm, 300 mm, 400 mm and 500 mm respectively; APDL codes developed and analyzed systematically.

Same procedure has been applied to the rectangular plates whose aspect ratio is 1 / 2 and also 1 / 3. The rectangular plates in this study are modelled with simply-supported boundary conditions on four sides.

The plate models are made out of steel according to ASTM A992, with density of ρ = 7.697e-8 N/mm^3, modulus of elasticity 199948 N/mm^2 and Poisson's ratio of 0.3.

The numbers of holes in models are dependent to sub model numbers and aspect ratios. This value can be calculated as aspect times 4n^2. For example if aspect ratio is 1 / 2 and model number is 3; there are 72 holes in perforated rectangular plate model.

Radii are constant and depends on "a" and for all aspect ratios it can be calculated with a/8n and hole locations are also different for every model.

Plate thickness is 1/150 of "a" value which is y dimension of rectangular plate so the analysis results were compared properly. Total surface areas of holes are exactly same for each model. For different plate length "a" 10 model with different number of holes are analyzed and normalized midpoint deflections respect to model numbers and plate width are presented.

In this study the effects of geometric discontinuities on perforated thin rectangular plates investigated. For each y dimension of the rectangular plate, when the number of holes increases the midpoint deflection also increases, but the total

hole area is equal for all sub models.

The variation of the midpoint deflections decrease asymptotically respect to number of holes after 7th sub model.

Midpoint deflections of the perforated rectangular plates are divided by their surface areas for all models and it is shown that these ratios are independent from the plate dimensions. So that designers can take into account these midpoint deflections of the plate by using these useful graphics.

REFERENCES

[1] S. Timoshenko and S. Woinowsky-Krieger, *Theory of Plates and Shells*, McGraw-Hill, Singapore, 1959.

[2] W.J. O'Donnell and B. F. Langer, "Design of perforated plates," *Journal of Engineering for Industry*, vol. 84, no. 3, pp. 307-319, 1962.

[3] A. Alshaya, J. Hunt, and R. Rowlands, "Stresses and strains in thick perforated orthotropic plates," *Journal of Engineering Mechanics*, vol. 142, no. 11, 2016.

[4] N. Kılıç, B. Ekici, and S. Bedir, "Optimization of high hardness perforated steel armor plates using finite element and response surface methods," *Mechanics of Advanced Materials and Structures*, vol. 24, no. 7, pp. 615-624, 2016.

[5] I. Radisavljevic, S. Balos, M. Nikacevic, and L. Sidjanin, "Optimization of geometrical characteristics of perforated plates," *Materials and Design*, vol. 49, pp. 81-89, 2013.

[6] H. Y. Woo, A. W. Leissa, and J. H. Kang, "Exact solutions for stresses, strains, displacements, and stress concentration factors of a perforated rectangular plate by a circular hole subjected to in-plane bending moment on two opposite edges," *Journal of Engineering Mechanics*, vol. 140, no. 6, 2013.

[7] C. W. Zhou, J. P. Pain é, M. N. Ichchou, and A. M. Zine, "Numerical and experimental investigation on broadband wave propagation features in perforated plates," *Mechanical Systems and Signal Processing*, vol. 75, pp. 556-575, 2016.

[8] M. Pedersen, W. Olthuis, and P. Bergveld, "On the mechanical behaviour of thin perforated plates and their application in silicon condenser microphones," *Sensors and Actuators A: Physical*, vol. 54, pp. 499-504, 1996.

[9] C. Atanasiu and S. T. Sorohan, "Displacements and stresses in bending of circular perforated plate," in *Proc. IOP Conf. Series: Materials Science and Engineering*, vol. 147, 2016.

[10] Y. Mei, M. Li, J. Song, and X. Gao, "Stress analysis of perforated plate based on ANSYS," *Advanced Materials Research*, pp. 652-654, 2013.

[11] M. H. Saraçoğlu and U. Albayrak, "Linear static analysis of perforated plates with round and staggered holes under their self-weights," *Res. Eng. Struct. Mat*., vol. 2, no. 1, pp. 39-47, 2016.

[12] M. H. Saraçoğlu and U. Albayrak, "Computational analysis of perforated rectangular thin plates," in *Proc. 2nd International Conference on Civil and Environmental Engineering*, 2017.

[13] D. Rood, *Theory and Analysis of Elastic Plates and Shells*, CRC Press-Taylor & Francis Group, Boca Raton, 2007.

[14] ANSYSInc., Release 10.0 Documentation for ANSYS, 2005.

[15] ANSYSInc., ANSYS commands reference, 2005.

[16] ANSYSInc., APDL programmer's guide, 2005.

Uğur Albayrak received his B.Sc in civil engineering, a M.Sc. in structural engineering and a PhD in structural engineering from Eskisehir Osmangazi University (ESOGU) Dept. of Civil Engineering, Turkey. He is presently working as an assistant professor at the same department. His main research interests include design of steel structures, R.C. structures, earthquake resistant design and computer applications in Civil Eng., and having more than 15 publications in national and international journals.

Mustafa Halûk Saraçoğlu received his MSc. in civil engineering from Dumlupınar University in 2002. He received his PhD. in civil engineering from Eskişehir Osmangazi University in 2010. His main scholarly interests are plates, laminated composites, matrix structural analysis, finite difference method, finite element method. Currently, he is an assistant professor at Dumlupınar University, Turkey.